Dental Materials Journal 2016; 35(2): 216–224

Comparative study on the resorbability and dissolution behavior of octacalcium phosphate, β-tricalcium phosphate, and hydroxyapatite under physiological conditions

Susumu SAKAI[1], Takahisa ANADA[1], Kaori TSUCHIYA[1], Hajime YAMAZAKI[2], Henry C. MARGOLIS[2] and Osamu SUZUKI[1]

[1] Division of Craniofacial Function Engineering, Tohoku University Graduate School of Dentistry, Sendai 980-8575, Japan
[2] Center for Biomineralization, Department of Applied Oral Sciences, The Forsyth Institute, Cambridge, MA 02142, USA
Corresponding author, Osamu SUZUKI; E-mail: suzuki-o@m.tohoku.ac.jp

The dissolution behaviors of octacalcium phosphate (OCP), β-tricalcium phosphate (β-TCP), and hydroxyapatite (HA) were compared by implanting the materials in rat subcutaneous pouches for 8 weeks using a filter chamber or immersing them in simulated body fluid (SBF) or Tris-HCl buffer for 2 weeks at pH 7.4 and 37°C. X-ray diffraction, Fourier transform infrared spectroscopy, scanning electron microscopy, and chemical analysis were conducted on these materials. Degree of supersaturation (DS) in the two solutions immersed with each calcium phosphate material was calculated from their chemical compositions. The results showed that OCP partially converted to apatitic crystals, while β-TCP and HA remained unchanged after the implantation. The DS of the SBF solution remained slightly supersaturated with respect to OCP and β-TCP, but slightly undersaturated in the Tris-HCl buffer. These findings suggest that previously reported OCP and β-TCP biodegradation could be induced through cell-mediated osteoclastic resorption rather than a simple dissolution process.

Keywords: Resorbability, Dissolution, Octacalcium phosphate, β-tricalcium phosphate, Hydroxyapatite

INTRODUCTION

Calcium phosphate materials have been extensively used to fill various bone defects in orthopedic and oral maxillofacial surgeries due to their superior osteoconductive properties[1]. The osteoconductivity is defined as a property of the material that provides a location where living bone can directly bond to the surface without any intervention of connective tissue[2]. On the other hand, calcium phosphate materials have also been classified depending on the resorbability[1,3]. Hydroxyapatite (HA), β-tricalcium phosphate (β-TCP), and octacalcium phosphate (OCP) exhibit bone bonding characteristics when implanted in bone defects[1,3-6]. However, HA does not show resorbability when it is fabricated through a sintering process and has a stoichiometric Ca/P molar ratio near 1.67[7]. Nevertheless, it becomes resorbable when it contains impurities, such as carbonate, structural defects, or its dimension is reduced to nano-scale[7-10], which results in a non-stoichiometric composition of HA. β-TCP and OCP have been classified as resorbable calcium phosphate materials and are expected to be replaced with newly formed bone[3,4,11].

The solubility isotherm of calcium phosphate phases previously reported indicates that it dissolves under a specific pH ranging from acidic to alkaline at room temperature[1,12]. Solubility is highest in dicalcium phosphate dihydrate (DCPD) and decreases in the order of OCP, β-TCP, and HA at physiologic pH 7.4 and 25°C[1,12-14]. However, this order does not always correspond to the resorption rate of these materials if they are placed in physiological conditions due to the presence of various bio-molecules and ions surrounding the crystals that regulate the dissolution and deposition of the calcium phosphate phases[15-19]. The solution compositions of serum and tissue fluid are known to be supersaturated with respect to HA and almost saturated with respect to OCP[20,21], thus allowing for newly formed HA crystals to deposit on implanted HA and OCP material surfaces[20,22,23]. One study has reported that β-TCP begins to dissolve below pH 6.2 based on a calculation from pH-controlled simulated body fluid[24]. Therefore, these studies suggest that OCP and β-TCP may not dissolve in a predictable fashion according to the solubility isotherm, under *in vivo* conditions.

OCP has been shown to biodegrade through osteoclastic resorption if implanted in various bone defects of murine and rabbit marrow spaces[25-27] and murine calvaria[28,29]. β-TCP has also been reported to undergo direct resorption by osteoclastic cells in rat bone marrow space[27,30] as well as human bone defects[31]. These studies and the above mentioned solubility study support the hypothesis that OCP and β-TCP may be directly resorbed by osteoclastic cells unless the pH around these calcium phosphate materials drops to a relatively acidic environment, which could be induced through inflammation[32]. In contrast, isolated osteoclastic cells can form a resorption pit on β-TCP and HA *in vitro*, but not on OCP[33].

OCP has been shown to enhance osteoclast formation *in vitro* through bone marrow cells in the presence of osteoblasts and the absence of active vitamin D_3, which is known to increase the osteoclast

Received Jul 27, 2015: Accepted Oct 8, 2015
doi:10.4012/dmj.2015-255 JOI JST.JSTAGE/dmj/2015-255

formation factor receptor activator of NF-kappa B ligand (RANKL) expression in osteoblasts[34]. OCP is a thermodynamically metastable phase that can be progressively hydrolyzed into HA at physiological pH[35,36]. The process of converting OCP to HA induces calcium consumption from and phosphate release into surrounding solutions around the crystals[12,37]. Thus, the change in calcium ion concentration around OCP crystals is probably highly associated with the induction of osteoclast formation from the co-culture environment[34]. However, there is still a paucity of data indicating how these calcium phosphates are dissolved and which factors of the materials regulate their dissolution under physiological conditions. The present study was investigated to elucidate how these biodegradable calcium phosphate materials dissolve under physiological conditions *in vitro* and *in vivo* from the view point of physicochemical changes of the materials. Special emphasis was placed on the resorption of OCP in comparison to two clinically approved and commercially widely used biomaterials, *β*-TCP and sintered non-resorbable HA in the absence of cells.

MATERIALS AND METHODS

Preparation of materials

OCP was synthesized by mixing calcium and phosphate solutions under a constant pH 5–6 and temperature at 70ºC according to a well-established wet synthesis method previously reported[6]. The precipitate was recovered from the reacting solution, washed with water several times, and dried at 105ºC for subsequent use. Sintered HA (Apaceram® G-S-5, HOYA Technosurgical, Tokyo, Japan) and sintered *β*-TCP (Osferion G2-5, Olympus Terumo Biomaterials, Tokyo, Japan) were commercially purchased. All of the materials were ground with an agate mortar and pestle and sieved to 300–500 μm with a standard testing sieve before being used in the experiments.

Characterization of materials

Calcium phosphate materials were characterized by X-ray diffraction (XRD) and Fourier transform infrared spectroscopy (FTIR). XRD patterns were recorded using a step scanning at 0.05 degree intervals from 3.0 degrees to 60.0 degrees, with Cu K*α* X-rays on a diffractometer (Mini Flex, Rigaku Electrical, Tokyo, Japan) at 30 kV and 15 mA. The theta range measurement included the main reflection (100) of OCP at 4.7º two theta. The Powder Diffraction File (PDF) card was utilized to identify their crystalline phases. The FTIR spectra of the materials were obtained by FTIR spectroscope (FT/IR-6300, JASCO, Tokyo, Japan) with the sample diluted in KBr over a range of 4,000–400 cm^{-1} with 4 cm^{-1} resolution. The morphologies of crystals and granules were examined using a JEOL analytical scanning electron microscope (SEM) JSM-6390LA (Tokyo, Japan) operating at an accelerating voltage of 10 kV. Au-Pd sputtering was performed using the powder samples before the observation.

Implantation of materials

A filter chamber was used to implant the materials in rat subcutaneous tissue for analysis of the dissolution under cell-free conditions. A polytetrafluoroethylene (PTFE) ring with an 11 mm outer diameter, 8 mm inner diameter, and 1 mm thickness (Nikkin, Osaka, Japan) was placed onto a 0.22 μm Millipore membrane using medical tissue glue (Aron Alpha A, Sankyo, Tokyo, Japan). Sterilized OCP (0.01 g), HA (0.05 g), and *β*-TCP (0.02 g) granules were placed inside the PTFE ring so as to fill the inside volume of the ring. Since the apparent density of materials varies, the weight of the materials filled in the ring resulted in the different value. In order to prevent an outflow of the granules, the ring was then covered with the same 0.22 μm Millipore membrane with glue as shown in Fig. 1. OCP was dried and sterilized at 105ºC for 24 h. The chamber filled with the granules of sterilized HA and *β*-TCP (as received) and the dried OCP, respectively, was further sterilized by irradiation in a UV-linker (FS-1500, Funakoshi, Tokyo, Japan) for 24 h before the use. Twelve-week-old male Wistar rats (SLC, Hamamatsu, Shizuoka, Japan) were used. The principles of laboratory animal care were followed as in the national laws. All procedures were approved by the Animal Research Committee of Tohoku University. The experimental rats were anesthetized with an intraperitoneal injection of sodium pentobarbital (50 mg/kg) supplemented with ether inhalation. The granules in the ring chamber sealed with a membrane were implanted into abdominal subcutaneous pouches. At 8 weeks post-implantation, the rats were anesthetized with an intraperitoneal injection of sodium pentobarbital (50 mg/kg) supplemented with ether inhalation. The rats were then sacrificed and the implants were retrieved for subsequent analyses.

Analyses of implanted granules

The retrieved granules from the filter chamber were dried at 60°C for 24 h (Dry Sterilizer STA420DA, Toyo Seisakusho Kaisha, Tokyo, Japan). The XRD, FTIR, and SEM analyses were performed under the same

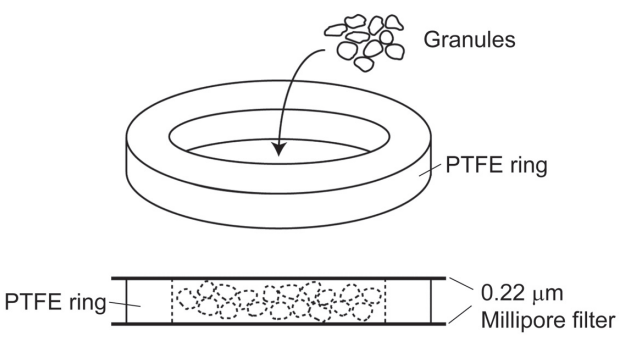

Fig. 1 Schematic diagram of the filter chamber for implanting the calcium phosphate materials in rat subcutaneous tissue to analyze the dissolution under cell-free conditions.

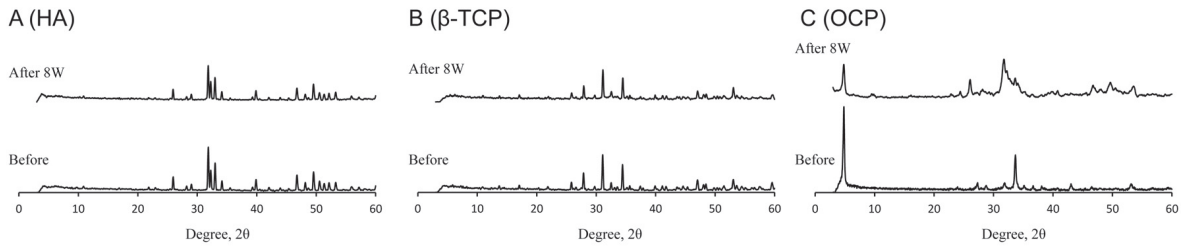

Fig. 2 Changes in the XRD pattern of HA (A), *β*-TCP (B), and OCP (C) granules before implantation and 8 weeks post-implantation in rat abdominal subcutaneous pouches.

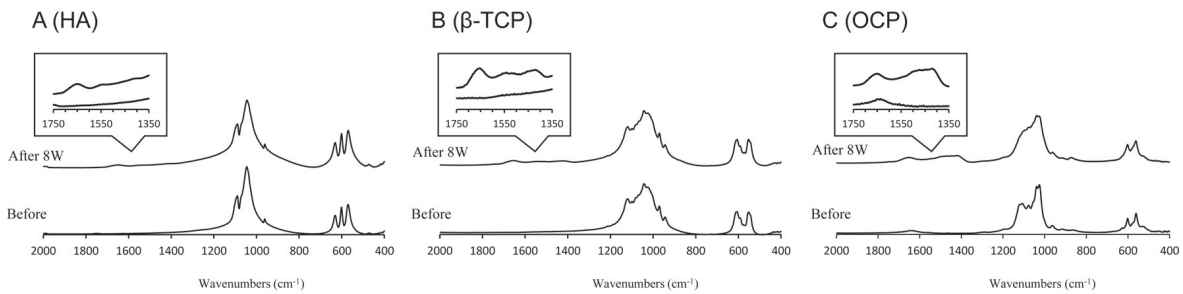

Fig. 3 Changes in the FTIR spectra of HA (A), *β*-TCP (B), and OCP (C) granules before implantation and 8 weeks post-implantation in rat abdominal subcutaneous pouches.
Spectra in the range from 1,350 cm^{-1} to 1,750 cm^{-1} was shown in the insertion of the respective materials.

conditions used for the characterization of the crystals as described above. The granules were dissolved in 1 M HCl to measure the calcium and phosphate ion concentrations by Calcium E tests and Phosphor C tests, respectively (Wako Pure Chemical Industries, Osaka, Japan), and the Ca/P molar ratios of the granules were calculated.

Immersion in simulated body fluid (SBF) solution and Tris-HCl buffer solution

SBF solution was prepared according to a previously described method[38] by dissolving reagent grade sodium chloride, sodium hydrogen carbonate, potassium chloride, dipotassium hydrogen phosphate trihydrate, magnesium chloride hexahydrate, and calcium chloride dihydrate in filtered purified water made by a Millipore Mill-Q Academic A10 (Millipore, Tokyo, Japan). The solution was then buffered with trihydroxymethyl aminomethane and hydrochloric acid to attain pH 7.4 at 37.0°C. Ion concentrations of 142, 148.8, 5, 1.5, and 4.2 mM of Na Cl, K, Mg, and HCO_3 were used for the SBF composition[38]. A Tris-HCl buffer solution (150 mM, pH 7.4) was also used as a comparative study. 50 mg of OCP, *β*-TCP and HA materials were immersed in 50 mL of the fresh SBF or Tris-HCl solutions in separate plastic tubes and kept at 37.0°C for 15 days. The immersed materials were collected after 1, 3, 7, 9, and 15 days for the SBF solution and 1, 4, 7, 9, and 15 days for the Tris-HCl solution. Those materials were washed with water several times and lyophilized for subsequent examination.

Chemical composition of SBF and Tris-HCl solutions after incubation with OCP, β-TCP, and HA and estimation of the saturation level

The degree of supersaturation (DS) values of SBF and Tris-HCl solutions after immersing OCP, *β*-TCP, and HA were calculated with respect to OCP, *β*-TCP, and HA in their supernatants. The DS values are the numerical values obtained by dividing the ion activity product for each calcium phosphate phase in solution by its respective solubility product constant. The solubility product constant corresponds to a pre-determined ion activity product at which the solution is saturated with respect to a specific calcium phosphate salt. DS values equal to 1.0, <1.0, and >1.0, represent conditions of saturation, undersaturation and supersaturation, respectively. The DS calculations were made for 37°C using a modification of ion speciation software previously developed[39,40] using the analytical concentrations of Ca, Mg, Na, K, P, Cl, and F as well as the pH value combined with the three mass balance equations for [Ca], [P], and [Mg][39,41,42]. The calculation also assumes the presence of HCO_3^- in the fluid. The ion pairs included in the calculation were $CaH_2PO_4^+$, $CaHPO_4^0$, $MgHPO_4^0$, $CaHCO_3^+$, and $MgHCO_3^+$. The DS was defined in terms of the mean ionic activity products with respect to HA, OCP, DCPD, and *β*-TCP. In the present study,

the concentrations of Ca^{2+} and inorganic phosphate ion obtained by chemical analyses were used for SBF. An ion concentration of 150 mM Na^+ as a substitute for the 150 mM Tris concentration and a pH value 7.4 were used for the calculation in Tris-HCl buffer solution. The solubility product constants used were 7.36×10^{-60} [mol/L][9] for HA[18], 2.51×10^{-49} [mol/L][8] for OCP[43], and 2.83×10^{-30} [mol/L][5] for β-TCP[44].

Statistical analysis

All values were reported as the means±standard deviations. All experiments were performed at least three times and showed reliable reproducibility.

RESULTS

Implantation of materials in rat abdominal subcutaneous pouches

The XRD analysis results of the granules in the chamber before implantation and 8 weeks post-implantation in rat abdominal subcutaneous pouches are shown in Fig. 2. The XRD patterns of the HA and β-TCP (Figs. 2A and B) remained unchanged during the 8 weeks implantation. On the other hand, the intensities of specific peaks (2θ=4.9° and 33.6°) of OCP were decreased after the 8 weeks implantation (Fig. 2C). Figure 3 shows the FTIR spectra of HA, β-TCP, and OCP before implantation and 8 weeks post-implantation in rat abdominal subcutaneous pouches. The spectra of β-TCP and OCP (Figs. 3B and C) after the 8 weeks implantation showed typical peaks of N-H bending vibration for amide II at 1,530 cm^{-1} and C=O stretching vibration for amide I at 1,630 cm^{-1} [45]. The spectra of β-TCP and OCP (Figs. 3B and C) after the 8 weeks implantation also showed typical peaks of ν_1 or ν_4 carbonate ion absorption at 1,410 cm^{-1} to 1,450 cm^{-1} [46,47]. These FTIR characteristic peaks were also recognized in HA although its intensity was lower than those in OCP and β-TCP (Fig. 3A). Furthermore, the characteristic peaks of OCP at 1,075 and 1,035 cm^{-1} became obscured after the 8 weeks implantation. Figure 4 shows scanning electron micrographs of HA, β-TCP, and OCP after the 8 weeks implantation. The morphology of HA crystals (Figs. 4A and D) remained unchanged by the implantation. The morphology of the β-TCP crystals (Figs. 4B and E) after the 8 weeks implantation also showed similar morphology to that before implantation but a small amount of deposits were recognized on the surface.

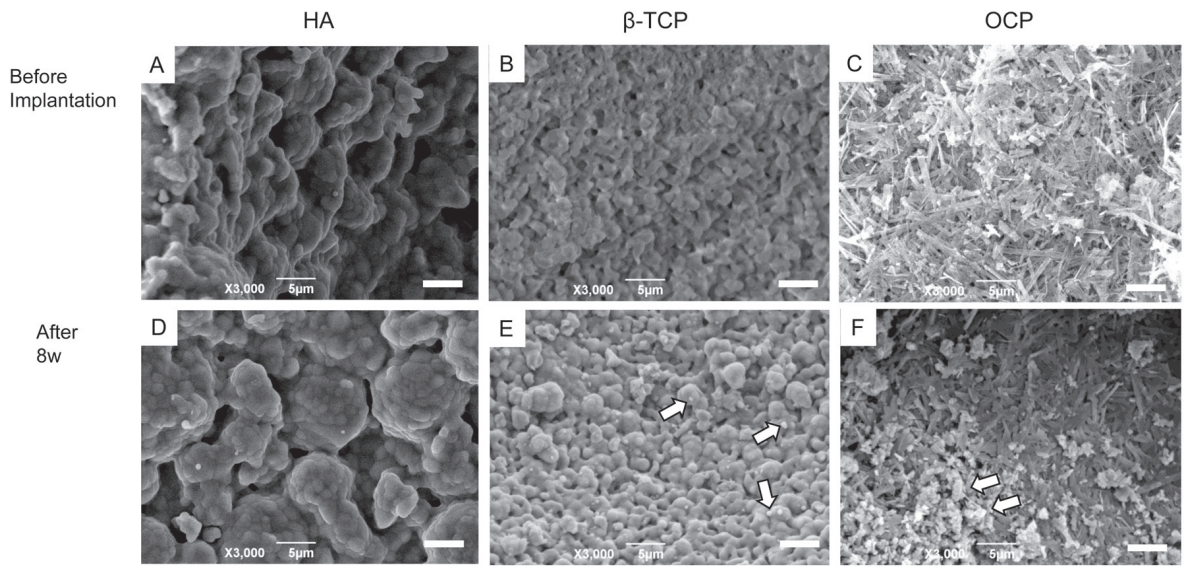

Fig. 4 Scanning electron micrographs of HA (A, D), β-TCP (B, E), and OCP (C, F) before implantation and 8 weeks post-implantation in rat abdominal subcutaneous pouches.
Bars=5 μm. Arrows: the particles considered as newly formed crystals.

Table 1 Ca/P molar ratios of materials before and after implantation for 8 weeks

	HA[a]	β-TCP[b]	OCP[c]
Before	1.62±0.01	1.45±0.04	1.30±0.01
After 8 weeks	1.60±0.01	1.46±0.01	1.49±0.03

[a]: n=5, [b]: n=3, [c]: n=3

The plate-like morphology of OCP crystals (Figs. 4C and F) remained relatively constant even at 8 weeks post-implantation, but also the micrographs showed smaller precipitates deposited on the OCP crystals. The Ca/P molar ratio of each material before and after the implantation was shown in Table 1. The Ca/P molar ratio of HA and β-TCP remained unchanged during the implantation. On the other hand, the Ca/P molar ratio of OCP increased after the implantation.

Immersion in SBF and Tris-HCl solutions

Figure 5 shows the XRD patterns and FTIR spectra of HA, β-TCP, and OCP before and after the immersion in Tris-HCl buffer up to 15 days. Figure 6 shows the XRD patterns and FTIR spectra of HA, β-TCP, and OCP before and after the immersion in SBF solution

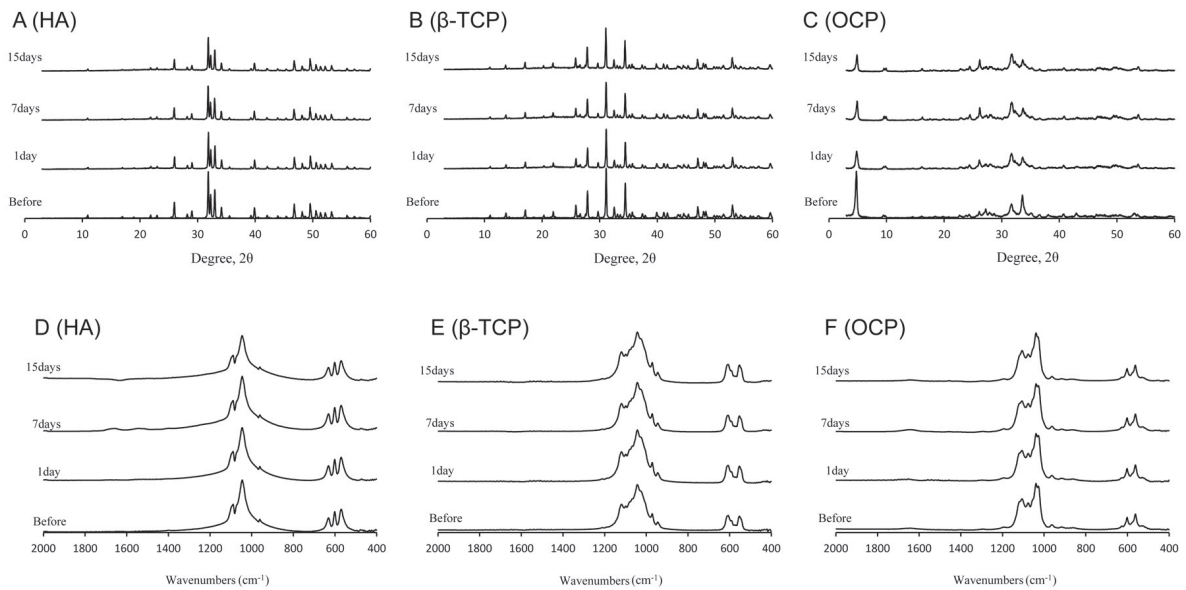

Fig. 5 Changes in the XRD pattern (A–C) and FTIR spectra (D–F) of granules before and after immersion in Tris-HCl buffer for up to 15 days.

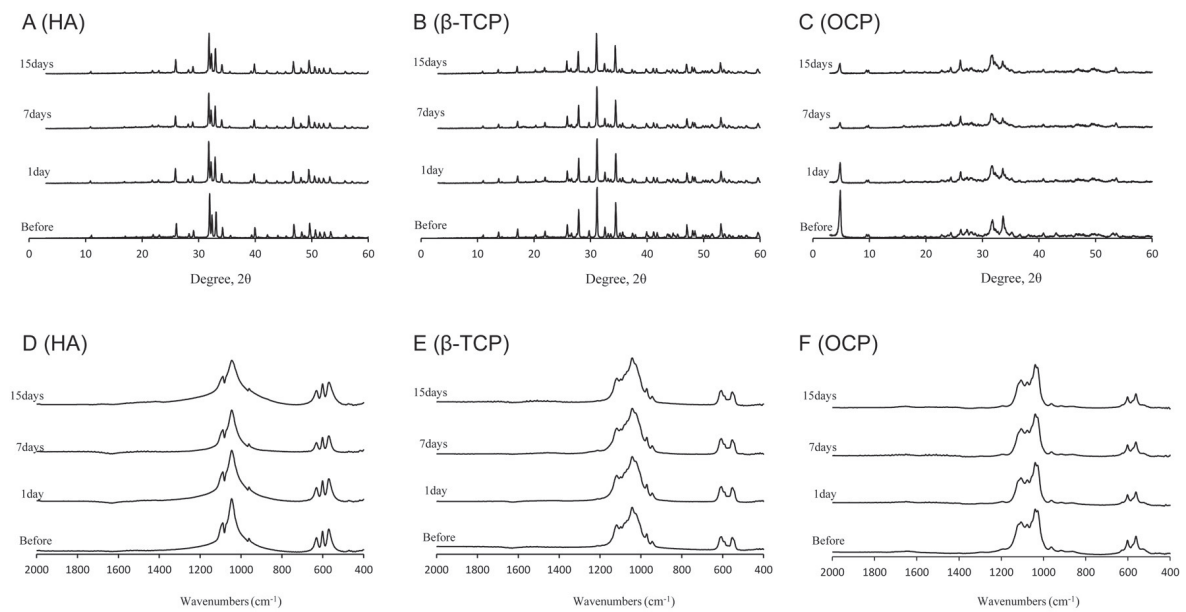

Fig. 6 Changes in the XRD pattern (A–C) and FTIR spectra (D–F) of granules before and after immersion in SBF solution for up to 15 days.

Table 2 Composition and saturation levels of SBF and Tris-HCl buffer solutions

Solutions/Crystals	Days	Conc. mM		DS at pH 7.40 and 37ºC			
		Calcium	Phosphate	HA	OCP	DCPD	β-TCP
SBF original	—	2.38	0.98	1.00×10^{12}	2.37×10^{3}	6.46×10^{-1}	1.98×10^{3}
	1	1.51	0.42	9.57×10^{9}	3.50×10^{1}	1.84×10^{-1}	1.03×10^{2}
HA	3	1.36	0.33	2.79×10^{9}	1.13×10^{1}	1.30×10^{-1}	4.70×10^{1}
	7	1.18	0.22	4.00×10^{8}	1.85×10^{0}	7.46×10^{-2}	1.34×10^{1}
	1	1.43	0.34	3.79×10^{9}	1.46×10^{1}	1.40×10^{-1}	5.66×10^{1}
β-TCP	3	1.30	0.30	1.68×10^{9}	7.09×10^{0}	1.13×10^{-1}	3.39×10^{1}
	7	1.12	0.16	1.29×10^{8}	6.30×10^{-1}	5.30×10^{-2}	6.43×10^{0}
	1	1.30	0.36	3.04×10^{9}	1.28×10^{1}	1.38×10^{-1}	5.04×10^{1}
OCP	3	1.14	0.29	8.00×10^{8}	3.84×10^{0}	9.62×10^{-2}	2.16×10^{1}
	7	1.05	0.22	2.35×10^{8}	1.22×10^{0}	6.73×10^{-2}	9.79×10^{0}
Tris-HCl original	—	0.032	0.0029	2.45×10^{-5}	4.07×10^{-12}	3.19×10^{-5}	6.89×10^{-8}
	1	0.083	0.034	4.47×10^{0}	2.90×10^{-7}	9.68×10^{-4}	1.62×10^{-4}
HA	4	0.086	0.032	4.69×10^{0}	2.91×10^{-7}	9.55×10^{-4}	1.65×10^{-4}
	7	0.10	0.018	1.86×10^{0}	9.80×10^{-8}	6.29×10^{-4}	8.42×10^{-5}
	1	0.29	0.18	3.09×10^{5}	5.82×10^{-3}	1.74×10^{-2}	1.81×10^{-1}
β-TCP	4	0.30	0.18	4.39×10^{5}	7.81×10^{-3}	1.88×10^{-2}	2.24×10^{-1}
	7	0.30	0.17	3.13×10^{5}	5.64×10^{-3}	1.70×10^{-2}	1.80×10^{-1}
	1	0.41	0.43	2.35×10^{7}	3.12×10^{-1}	5.85×10^{-2}	2.89×10^{0}
OCP	4	0.38	0.46	1.94×10^{7}	2.79×10^{-1}	5.78×10^{-2}	2.61×10^{0}
	7	0.41	0.43	2.40×10^{7}	3.19×10^{-1}	5.90×10^{-2}	2.93×10^{0}

up to 15 days. The FTIR spectra of HA and β-TCP remained unchanged after immersion in both solution. The characteristic peaks of OCP at 1,075 and 1,035 cm^{-1} became slightly broadened up to 15 day period. The XRD patterns of HA and β-TCP also remained unchanged after immersion in both solution. The intensity of primary peak of OCP at 2θ=4.9º decreased over time in both solutions.

Solubility of OCP, β-TCP, and HA estimated by the degree of supersaturation

The additions of calcium phosphate materials into the supersaturated SBF solution induced decreases in calcium and phosphate concentrations at 1 day which eventually resulted in similar concentrations at 7 days. This is most likely due to the precipitation of calcium phosphates, most probably HA, upon the introduction of calcium phosphate materials into the SBF solution, as detected especially by changes in the XRD pattern of OCP. SBF was stable without addition of the materials at least experimental period 7 days. The DS values of the supernatants are summarized in Table 2. The initial SBF solution without the calcium phosphate materials has a composition that was highly supersaturated with respect to HA, supersaturated with respect to OCP and β-TCP, but undersaturated with respect to DCPD. All of the DS values with respect to HA decreased upon the introduction of each of the three calcium phosphate crystals to the SBF solution, although it remained supersaturated even after 7 days. The DS values of the solutions immersed with HA and OCP crystals became saturated with respect to OCP. The DS values of the solution immersed with β-TCP crystals remained slightly supersaturated with respect to β-TCP. All of the DS values with respect to DCPD remained undersaturated throughout the immersion periods. DS values of initial Tris-HCl buffer without the calcium phosphate materials were estimated to be undersaturated with respect to all of the phases due to the lack of calcium and phosphate ions in the solution. The DS values of the solution immersed with the HA crystals became saturated with respect to HA, but remained undersaturated with respect to OCP, DCPD, and β-TCP. The DS values of the solutions immersed with OCP crystals became supersaturated with respect to HA but remained undersaturated with respect to OCP and DCPD and saturated with respect to β-TCP until 7 days. On the other hand, the DS values of the solutions immersed with β-TCP crystals became supersaturated with respect to HA but remained undersaturated with respect to OCP, DCPD and β-TCP even after 7 days.

DISCUSSION

The present study provides evidence that OCP reacted with tissue fluid to partially transform its structure

into HA in an *in vivo* subcutaneous implantation. On the other hand, although the implanted HA and *β*-TCP did not show substantial change in the structure, FTIR analysis detected carbonate ions and amide absorptions which were also detected more markedly in implanted OCP. It is well recognized that HA materials do not exhibit biodegradable properties because this phase is thermodynamically stable at neutral pH[1,12], and the sintering process further increases its chemical stability, in general, by diminishing inherent structural defects. Although HA is usually considered to be the prototype in bone apatite crystals[48-51], bone apatite crystals include impurities, such as carbonate, and have structural defects[48-51], which make it less stable in comparison to synthetic sintered HA[7].

The present study used the calcium phosphate materials with granule diameter of 300–500 μm for purposes described below. We have previously studied and characterized the effects of OCP granule size (*i.e.*, in the range of 53–300 and 500–1,000 μm) on their bone regenerative properties[29]. The osteoconductivity of OCP with a granule diameter of 300-500 μm has been extensively examined in previous studies[5,26,27,29,52]. Therefore, the present study also used a granule diameter of 300–500 μm in order to make comparison to these previous studies and establish a linkage in scientific knowledge between bone regeneration properties and the physicochemical characteristics.

A filter membrane used in the present study has been applied in order to allow the diffusion of the tissue fluid but blocking the cells to go through. In fact, the membrane implanted into rat calvaria with OCP granules has been used to isolate OCP granules from osteoblastic cells while the tissue fluid can inflow inside the membrane[53]. The physicochemical changes observed in the calcium phosphate materials in the present study can therefore be interpreted as the consequence of chemical reactions between tissue fluid components and the materials. Our preliminary study showed that sodium chloride salt is easily soluble in the filter chamber in one day after the implantation in subcutaneous pouches, indicating that the tissue fluid easily flows within the filter chamber. Moreover, the calcium phosphate granules are exposed to the physiological environment in the absence of the cell components.

Based on XRD analyses, HA and *β*-TCP structures remained unchanged, while OCP transformed partially into HA, if implanted. These trends were also confirmed by the chemical analyses that showed that while the Ca/P molar ratios of HA and *β*-TCP remained unchanged, the molar ratio of OCP increased from 1.30 to 1.49. This final Ca/P molar ratio was lower than that of the stoichiometric HA composition (1.67), suggesting that the partial hydrolysis and transformation of OCP to HA[5,54,55]. Furthermore, FTIR absorptions around 1,400 cm^{-1} to 1,600 cm^{-1} were detected for OCP. Similar absorption bands were also observed for both HA and *β*-TCP materials although their intensities were smaller than those seen with OCP. The FTIR features could be derived from the absorption of carbonate ions and amides of the proteins from the tissue fluid, or through the formation of carbonate apatite crystals on the material surfaces[46,47,54-56]. SEM analysis showed no remarkable changes in the morphology of HA, although OCP granules seemed to exhibit a deposition of newly formed and very small crystals, *β*-TCP granules also seemed to have small amount of mineral deposition, which may again correspond to formation of carbonate apatite crystals[23,56].

The *in vitro* immersion experiments in SBF and Tris-HCl solutions provided an indication of the chemical behavior of the materials during the *in vivo* implantation. The structural changes of *β*-TCP and HA were not clearly substantiated by XRD, while the OCP (100) peaks at 4.8° decreased with immersion in both SBF and Tris-HCl buffer solutions. However, analyses showed that the SBF solution immersed with OCP and *β*-TCP became slightly supersaturated with respect to OCP and *β*-TCP, whereas the Tris-HCl solution was found to be undersaturated with respect to OCP and *β*-TCP. HA (100) peaks around 2-theta=11° were not substantiated by XRD, which may be due to the dissolution of OCP without HA formation, or possibly to lower intensities of peaks expected in formed HA with low crystallinity. It has been reported that OCP has a potential role to form a bridge between bone mineral crystals by forming OCP-citrate-like hydrated layers during hydrolysis[57]. It is probable that the citrate ions could work to form such an intercalated structure in the present *in vivo* hydrolysis of OCP although XRD and FTIR analyses did not detect clear evidence for such a structure. Taken together, the reduction of OCP (100) peak may correspond to the partial conversion to HA in SBF immersion in the same way as *in vivo* implantation but to the simple dissolution in Tris-buffer immersion. The solution immersed with HA remained supersaturated with respect to HA in SBF and almost saturated with respect to HA in Tris-HCl. The SBF immersion results corresponded well with the dissolution tendency shown in the *in vivo* analyses and indicated that OCP and *β*-TCP do not dissolve under physiological conditions where calcium and phosphate preexist, which is consistent with previous estimations of solubility[20,21,24,58]. A question has been posed regarding the stability of SBF in relation to the formation of HA, which could be related to its level of supersaturation, regardless of the presence of the calcium phosphate materials[59]. Our previous study confirmed that the DS value of the medium immersed with OCP remained slightly supersaturated with respect to OCP[60] , as also seen in the present study. The histologic analysis has shown that biodegradation of OCP and *β*-TCP is accompanied by osteoclastic resorption if implanted in bone defects[27,30]. It has been reported that the biodegradation rate of OCP is higher than *β*-TCP if they were implanted in rat tibia for 8 weeks[27,30]. Results of the present study indicate that OCP and *β*-TCP cannot be resorbed in the absence of cellular components in the presence of suitable amounts of calcium and phosphate ions. These findings suggest that both

OCP and β-TCP are biodegraded primarily through cell-mediated osteoclastic resorption, and not through simple physicochemical dissolution. Moreover, the higher prevailing resorption rate of OCP compared to β-TCP[27] may be also driven by the capability of OCP to enhance osteoclast formation[34].

CONCLUSION

The present study compared the resorbability of OCP and β-TCP to that of HA in relation to their physicochemical properties. The OCP phase tended to convert to HA while those of β-TCP and HA remained unchanged, although carbonate and protein absorption were detected by FTIR analysis. DS values of the SBF solution immersed with three materials remained supersaturated with respect to these phases. The results from the *in vitro* experiments can explain the resorbable properties of these calcium phosphate materials implanted *in vivo* tissues. The results obtained further suggest that OCP and β-TCP could be resorbed through cell-mediated osteoclastic resorption, rather than a simple dissolution process, as would be anticipated from solubility considerations, as previously reported.

ACKNOWLEDGMENTS

This study was supported by Grants-in Aid (23106010, 23390450 and 25670829) from the Ministry of Education, Science, Sports, and Culture of Japan.

REFERENCES

1) Chow LC. Next generation calcium phosphate-based biomaterials. Dent Mater J 2009; 28: 1-10.
2) Hench LL, Wilson J. Surface-active biomaterials. Science 1984; 226: 630-636.
3) Kamitakahara M, Ohtsuki C, Miyazaki T. Behavior of ceramic biomaterials derived from tricalcium phosphate in physiological condition. J Biomater Appl 2008; 23: 197-212.
4) Oyane A, Wang X, Sogo Y, Ito A, Tsurushima H. Calcium phosphate composite layers for surface-mediated gene transfer. Acta Biomater 2012; 8: 2034-2046.
5) Suzuki O, Kamakura S, Katagiri T, Nakamura M, Zhao B, Honda Y, Kamijo R. Bone formation enhanced by implanted octacalcium phosphate involving conversion into Ca-deficient hydroxyapatite. Biomaterials 2006; 27: 2671-2681.
6) Suzuki O, Nakamura M, Miyasaka Y, Kagayama M, Sakurai M. Bone formation on synthetic precursors of hydroxyapatite. Tohoku J Exp Med 1991; 164: 37-50.
7) LeGeros RZ. Calcium phosphate-based osteoinductive materials. Chem Rev 2008; 108: 4742-4753.
8) Kikuchi M, Itoh S, Ichinose S, Shinomiya K, Tanaka J. Self-organization mechanism in a bone-like hydroxyapatite/collagen nanocomposite synthesized in vitro and its biological reaction in vivo. Biomaterials 2001; 22: 1705-1711.
9) Matsuura A, Kubo T, Doi K, Hayashi K, Morita K, Yokota R, Hayashi H, Hirata I, Okazaki M, Akagawa Y. Bone formation ability of carbonate apatite-collagen scaffolds with different carbonate contents. Dent Mater J 2009; 28: 234-242.
10) Nagayama M, Takeuchi H, Doi Y. Comparison of carbonate apatite and beta-tricalcium phosphate (resorbable calcium phosphates) implanted subcutaneously into the back of rats. Dent Mater J 2006; 25: 219-225.
11) Suzuki O. Octacalcium phosphate: osteoconductivity and crystal chemistry. Acta Biomater 2010; 6: 3379-3387.
12) Brown WE, Mathew M, Tung MS. Crystal chemistry of octacalcium phosphate. Prog Crystal Growth Charact 1981; 4: 59-87.
13) Christoffersen MR, Christoffersen J, Kibalczyc W. Apparent solubilities of two amorphous calcium phosphates and of octacalcium phosphate in the temperature range 30–42°C. J Cryst Growth 1990; 106: 349-354.
14) Vereecke G, Lemaître J. Calculation of the solubility diagrams in the system $Ca(OH)_2$-H_3PO_4-KOH-HNO_3-CO_2-H_2O. J Cryst Growth 1990; 104: 820-832.
15) Aoba T, Moreno EC, Shimoda S. Competitive adsorption of magnesium and calcium ions onto synthetic and biological apatites. Calcif Tissue Int 1992; 51: 143-150.
16) Boskey AL, Spevak L, Doty SB, Rosenberg L. Effects of bone CS-proteoglycans, DS-decorin, and DS-biglycan on hydroxyapatite formation in a gelatin gel. Calcifi Tissue Int 1997; 61: 298-305.
17) Gajjeraman S, Narayanan K, Hao J, Qin C, George A. Matrix macromolecules in hard tissues control the nucleation and hierarchical assembly of hydroxyapatite. J Biol Chem 2007; 282: 1193-1204.
18) Moreno EC, Kresak M, Zahradnik RT. Fluoridated hydroxyapatite solubility and caries formation. Nature 1974; 247: 64-65.
19) Tartaix PH, Doulaverakis M, George A, Fisher LW, Butler WT, Qin C, Salih E, Tan M, Fujimoto Y, Spevak L, Boskey AL. In vitro effects of dentin matrix protein-1 on hydroxyapatite formation provide insights into in vivo functions. J Biol Chem 2004; 279: 18115-18120.
20) Eidelman N, Chow L, Brown W. Calcium phosphate phase transformations in serum. Calcif Tissue Res 1987; 41: 18-26.
21) Eidelman N, Chow LC, Brown WE. Calcium phosphate saturation levels in ultrafiltered serum. Calcif Tissue Int 1987; 40: 71-78.
22) Daculsi G, LeGeros RZ, Heughebaert M, Barbieux I. Formation of carbonate-apatite crystals after implantation of calcium phosphate ceramics. Calcif Tissue Int 1990; 46: 20-27.
23) Suzuki O, Imaizumi H, Kamakura S, Katagiri T. Bone regeneration by synthetic octacalcium phosphate and its role in biological mineralization. Curr Med Chem 2008; 15: 305-313.
24) Toya H, Ito A, Fujimori H, Goto S, Ioku K. In vitro estimation of calcium phosphate with pH-controlled simulated body fluid. Trans Mater Res Soc Jpn 2001; 26: 1247-1250.
25) Imaizumi H, Sakurai M, Kashimoto O, Kikawa T, Suzuki O. Comparative study on osteoconductivity by synthetic octacalcium phosphate and sintered hydroxyapatite in rabbit bone marrow. Calcif Tissue Int 2006; 78: 45-54.
26) Kamakura S, Sasano Y, Homma-Ohki H, Nakamura M, Suzuki O, Kagayama M, Motegi K. Multinucleated giant cells recruited by implantation of octacalcium phosphate (OCP) in rat bone marrow share ultrastructural characteristics with osteoclasts. J Electron Microsc 1997; 46: 397-403.
27) Miyatake N, Kishimoto KN, Anada T, Imaizumi H, Itoi E, Suzuki O. Effect of partial hydrolysis of octacalcium phosphate on its osteoconductive characteristics. Biomaterials 2009; 30: 1005-1014.
28) Kikawa T, Kashimoto O, Imaizumi H, Kokubun S, Suzuki O. Intramembranous bone tissue response to biodegradable octacalcium phosphate implant. Acta Biomater 2009; 5: 1756-1766.
29) Murakami Y, Honda Y, Anada T, Shimauchi H, Suzuki O. Comparative study on bone regeneration by synthetic octacalcium phosphate with various granule sizes. Acta Biomater 2010; 6: 1542-1548.

30) Kondo N, Ogose A, Tokunaga K, Ito T, Arai K, Kudo N, Inoue H, Irie H, Endo N. Bone formation and resorption of highly purified beta-tricalcium phosphate in the rat femoral condyle. Biomaterials 2005; 26: 5600-5608.
31) Ogose A, Kondo N, Umezu H, Hotta T, Kawashima H, Tokunaga K, Ito T, Kudo N, Hoshino M, Gu W, Endo N. Histological assessment in grafts of highly purified beta-tricalcium phosphate (OSferion) in human bones. Biomaterials 2006; 27: 1542-1549.
32) Lardner A. The effects of extracellular pH on immune function. J Leukocyte Biol 2001; 69: 522-530.
33) Doi Y, Iwanaga H, Shibutani T, Moriwaki Y, Iwayama Y. Osteoclastic responses to various calcium phosphates in cell cultures. J Biomed Mater Res 1999; 47: 424-433.
34) Takami M, Mochizuki A, Yamada A, Tachi K, Zhao B, Miyamoto Y, Anada T, Honda Y, Inoue T, Nakamura M, Suzuki O, Kamijo R. Osteoclast differentiation induced by synthetic octacalcium phosphate through RANKL expression in osteoblasts. Tissue Eng Part A 2009; 15: 3991-4000.
35) LeGeros RZ, Daculsi G, Orly I, Abergas T, Torres W. Solution-mediated transformation of octacalcium phosphate (OCP) to apatite. Scanning Electron Microsc 1989; 3: 129-138.
36) Tomazic BB, Tung MS, Gregory TM, Brown WE. Mechanism of hydrolysis of octacalcium phosphate. Scanning Microsc 1989; 3: 119-127.
37) Suzuki O, Kamakura S, Katagiri T. Surface chemistry and biological responses to synthetic octacalcium phosphate. J Biomed Mater Res B Appl Biomater 2006; 77: 201-212.
38) Kokubo T, Kushitani H, Sakka S, Kitsugi T, Yamamuro T. Solutions able to reproduce in vivo surface-structure changes in bioactive glass-ceramic A-W. J Biomed Mater Res 1990; 24: 721-734.
39) Aoba T, Moreno EC. The enamel fluid in the early secretory stage of porcine amelogenesis: chemical composition and saturation with respect to enamel mineral. Calcif Tissue Int 1987; 41: 86-94.
40) Moreno EC, Margolis HC. Composition of human plaque fluid. J Dent Res 1988; 67: 1181-1189.
41) Moreno EC, Aoba T. Calcium bonding in enamel fluid and driving force for enamel mineralization in the secretory stage of amelogenesis. Adv Dent Res 1987; 1: 245-251.
42) Moreno EC, Aoba T. Comparative solubility study of human dental enamel, dentin, and hydroxyapatite. Calcif Tissue Int 1991; 49: 6-13.
43) Tung MS, Eidelman N, Sieck B, Brown WE. Octacalcium phosphate solubility product from 4 to 37 °C. J Res Nat Bur Stand 1988; 93: 613-624.
44) Gregory TM, Moreno EC, Patel JM, WE B. Solubility of β-$Ca_3(PO_4)_2$ in the system $Ca(OH)_2$-H_3PO_4-H_2O at 5, 15, 25 and 37 °C. J Res Natl Bur Stand 1974; 78A: 667-674.
45) Cataldo F, Ursini O, Lilla E, Angelini G. Radiation-induced crosslinking of collagen gelatin into a stable hydrogel. J Radioanal Nucl Chem 2008: 125-131.
46) Aoba T, Moreno EC. Changes in the nature and composition of enamel mineral during porcine amelogenesis. Calcif Tissue Int 1990; 47: 356-364.
47) Yokota R, Hayashi H, Hirata I, Miake Y, Yanagisawa T, Okazaki M. Detailed consideration of physicochemical properties of CO_3 apatites as biomaterials in relation to carbonate content using ICP, X-ray diffraction, FT-IR, SEM, and HR-TEM. Dent Mater J 2006; 25: 597-603.
48) Brown WE. Crystal growth of bone mineral. Clin Orthop Relat Res 1966; 44: 205-220.
49) Nelson DG, Featherstone JD. Preparation, analysis, and characterization of carbonated apatites. Calcif Tissue Int 1982; 34 Suppl 2: S69-81.
50) Simpson DR. Problems of the composition and structure of the bone minerals. Clin Orthop Relat Res 1972; 86: 260-286.
51) Young RA. Implications of atomic substitutions and other structural details in apatites. J Dent Res 1974; 53: 193-203.
52) Kobayashi K, Anada T, Handa T, Kanda N, Yoshinari M, Takahashi T, Suzuki O. Osteoconductive property of a mechanical mixture of octacalcium phosphate and amorphous calcium phosphate. ACS Appl Mater Interfaces 2014; 6: 22602-22611.
53) Sasano Y, Kamakura S, Nakamura M, Suzuki O, Mizoguchi I, Akita H, Kagayama M. Subperiosteal implantation of octacalcium phosphate (OCP) stimulates both chondrogenesis and osteogenesis in the tibia, but only osteogenesis in the parietal bone of a rat. Anat Rec 1995; 242: 40-46.
54) Chickerur NS, Tung MS, Brown WE. A mechanism for incorporation of carbonate into apatite. Calcif Tissue Int 1980; 32: 55-62.
55) Suzuki O, Yagishita H, Yamazaki M, Aoba T. Adsorption of bovine serum albumin onto octacalcium phosphate and Its hydrolyzates. Cell Mater 1995; 5: 45-54.
56) Suzuki Y, Kamakura S, Honda Y, Anada T, Hatori K, Sasaki K, Suzuki O. Appositional bone formation by OCP-collagen composite. J Dent Res 2009; 88: 1107-1112.
57) Davies E, Müller KH, Wong WC, Pickard CJ, Reid DG, Skepper JN, Duer MJ. Citrate bridges between mineral platelets in bone. Proc Natl Acad Sci USA 2014; 111: E1354-E1363.
58) Yokoi T, Kim IY, Ohtsuki C. Mineralization of calcium phosphate on octacalcium phosphate in a solution mimicking in vivo conditions. Phosphorus Res Bull 2012; 26: 71-76.
59) Bohner M, Lemaitre J. Can bioactivity be tested in vitro with SBF solution? Biomaterials 2009; 30: 2175-2179.
60) Kawai T, Anada T, Honda Y, Kamakura S, Matsui A, Matsui K, Echigo S, Suzuki O. Analysis of osteoblastic cell differentiation by synthetic octacalcium phosphate (OCP) as compared with commercially available β-TCP ceramic. Jpn J Oral Maxillofac Surg 2010; 56: 2-8.